Turbulence Modeling and the Physics of the Intra-Cluster Medium

Luigi Iapichino, Jens C. Niemeyer, Surajit Paul, and Wolfram Schmidt

Abstract The effective modeling of the stirring and development of turbulent flows in grid-based hydrodynamical simulations is computationally challenging. Here we present two possible ways to tackle the problem: first, we consider the use of the adaptive mesh refinement (AMR), applying novel refinement criteria which are optimized to follow the evolution of a turbulent flow. In a second step, the AMR is combined with a subgrid scale (SGS) model for the unresolved turbulence, thus resulting in a new numerical technique called *FEARLESS* (Fluid mEchanics with Adaptively Refined Large Eddy SimulationS). *FEARLESS* performs both the adaptive refinement of the regions where turbulent flows develop and a consistent coupling of the SGS turbulence with the resolved scales, and is argued to be a suitable tool in simulations of turbulent clumped flows. The results of galaxy cluster simulations, performed with the new tool, give rise to several interesting implications with regard to the physics of these objects, and to the numerical methods employed for their exploration in computational cosmology.

Luigi Iapichino
Zentrum für Astronomie der Universität Heidelberg, Institut für Theoretische Astrophysik, Albert-Ueberle-Str. 2, D-69120 Heidelberg, Germany
e-mail: luigi@ita.uni-heidelberg.de

Jens C. Niemeyer · Wolfram Schmidt
Institut für Astrophysik, Universität Göttingen, Friedrich-Hund-Platz 1, D-37077 Göttingen, Germany
e-mail: niemeyer@astro.physik.uni-goettingen.de
e-mail: schmidt@astro.physik.uni-goettingen.de

Surajit Paul
The Inter-University Centre for Astronomy and Astrophysics, Pune University Campus, Pune 411 007, India
e-mail: surajit@iucaa.ernet.in

S. Wagner et al. (eds.), *High Performance Computing in Science and Engineering, Garching/Munich 2009*, DOI 10.1007/978-3-642-13872-0_32,
© Springer-Verlag Berlin Heidelberg 2010

1 Introduction

The build-up of the cosmic structure, which proceeds through the process of hierarchical clustering [1], plays a key role for the conversion of potential gravitational energy into kinetic and internal energy in galaxy clusters and groups. In this process, cluster mergers induce bulk motions in the intra-cluster medium (henceforth ICM), with velocities of the order of 1000 km s^{-1} [2]. In this flow the gas bulk velocity is transonic and shocks are ubiquitous, thus the development and dissipation of turbulent gas motions can provide a non-negligible contribution to the energy budget.

The turbulent nature of the flow in the ICM will be directly probed with the help of high-resolution X-ray spectroscopy of emission line broadening by the next generation of X-ray telescopes [3–6]. At the present time, there is a number of observational clues that have been interpreted as evidence for the turbulent state of the ICM (see [7], for a review). In addition to the observations, there are many astrophysical problems that could benefit from a deeper theoretical knowledge of turbulence in the ICM such as the amplification of magnetic fields [8–10], the non-thermal emission in clusters [11], and the acceleration of cosmic rays [12–14], to name a few.

From the computational viewpoint, the evolution of the cosmic structure is the typical problem whose prominent features (complexity, nonlinearity and lack of symmetry) call for the use of numerical simulations as a central investigation tool. The wide range of length scales involved in the process makes the Smoothed Particle Hydrodynamics (SPH) technique very suitable and popular in the field, but grid codes, especially when coupled with the Adaptive Mesh Refinement (AMR), are also able to catch a significant part of the scales needed for properly modeling the clustering [15], and allow a complementary and less problematic approach to the baryonic processes [16, 17].

The formation and evolution of the cosmological large scale structure is therefore a case of turbulence generation in a strongly clumped medium. Some authors of this report (L.I., J.C.N., W.S.) are part of the research team which developed a new numerical method, called *FEARLESS* (Fluid mEchanics with Adaptively Refined Large Eddy SimulationS), that combines AMR with Large Eddy Simulations (LES) for the modelling of subgrid scale (SGS) turbulence. With the combined use of grid refinement and SGS model, *FEARLESS* is very suitable for simulations of intermittent turbulent flows in clumped media.

FEARLESS has been developed as part of this research project *h0973: Modelling of turbulent flows applied to numerical simulations of galaxy clusters*, focused on the physics of galaxy clusters, and of the companion project *h0972: Star formation in the turbulent interstellar medium and its implications on galaxy evolution*, devoted to the galactic scales. In this report we will briefly present the basic ideas of turbulence modelling through AMR and LES (Sect. 2), and then the results of our project *h0973* will be presented. In particular, we will review our works, and the related technical and computational issues, on mesh refinement techniques for resolving turbulent flows (Sect. 3), and the first application of the full FEARLESS approach to cluster simulations (Sect. 4). Finally in Sect. 5 the conclusion will be drawn, and some upcoming work will be sketched.

2 Numerical Tools for the Modeling of Turbulent Flows

FEARLESS arises from the combined use of adaptive mesh refinement (AMR) and a subgrid scale (SGS) model for the unresolved scales. This novel tool has been successfully implemented into the ENZO[1] code, v. 1.0 [18], an AMR, grid-based hybrid (hydrodynamics plus N-Body) code based on the PPM solver [19] modified for the study of cosmology [20], which provides the necessary infrastructure for performing numerical simulations of cosmological structure formation.

In the first phase of the project (cf. [21]) the development work was aimed on the AMR, in particular on refinement criteria which are best suited for refining turbulent flows. One such criterion was introduced in [22], and is based on the regional variability of structural invariants of the flow, i.e. variables related to the spatial derivatives of the flow velocity. An examples is the modulus of the vorticity $\omega = \nabla \times \mathbf{v}$ (the curl of the velocity field), expected to become high in regions where the flow is turbulent. The regional threshold for triggering the refinement is expressed in the comparison of the cell value of the variable $q(\mathbf{x},t)$ and the average and the standard deviation of q, calculated on a local grid patch:

$$q(\mathbf{x},t) \geq \langle q \rangle_i(t) + \alpha \lambda_i(t) \tag{1}$$

where λ_i is the maximum between the average $\langle q \rangle$ and the standard deviation of q in the grid patch i, and α is a tunable parameter.

This technique has been used in the simulations in [7, 23, 24], and we refer to Sect. 3 for their most relevant results.

In the case of astrophysically relevant Reynolds numbers, even using AMR one cannot resolve all the relevant length scales down to the dissipative one [25]. This is the case also in the case of galaxy clusters, which have to be followed in their evolution in large cosmological volumes, although the Reynolds number in the ICM is supposed to be only moderately high ([7, 26] for a review). In engineering applications as well as other fields of computational fluid dynamics, SGS models have been developed in order to account for the influence of unresolved turbulence on the resolved scales. This technique is often referred to as Large Eddy Simulations (LES) [27].

As shown by [25], the dynamics equations of a compressible, viscous, self-gravitating fluid can be decomposed into large-scale (resolved) and small-scale (unresolved) parts, using the filter formalism proposed by [28]. By means of filtering, any field quantity a can be split into a smoothed part $\langle a \rangle$ and a fluctuating part a', where $\langle a \rangle$ varies only at scales greater than the prescribed filter length. Following this procedure one can define the turbulent energy e_t, which can be visualized as an subgrid energy buffer between the resolved kinetic energy and the internal energy (graphically shown in Fig. 1). The turbulent energy is governed by an equation in the following form:

$$\frac{\partial}{\partial t}\langle \rho \rangle e_t + \frac{\partial}{\partial r_j}\hat{v}_j \langle \rho \rangle e_t = D + \Sigma + \Gamma - \langle \rho \rangle (\lambda + \varepsilon)\,, \tag{2}$$

[1] ENZO homepage: http://lca.ucsd.edu/software/enzo/

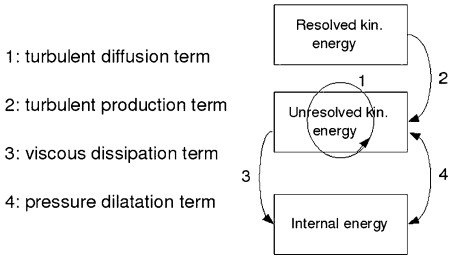

Fig. 1 Graphical description of the energy budget in *FEARLESS*, showing the three energy components and the exchange terms between them

where ρ is the gas density and $\hat{v}_j$ is the density-weighted filtered velocity component, according to Favre [29]. The quantities at the right-hand side of Eq. 2 determine the evolution of e_t and are the turbulent diffusion term D, the turbulent production term Σ, the pressure dilatation term λ and the viscous dissipation term ε. Their role in the energy budget is visually described in Fig. 1, and the way they are modelled (i.e. their closures) represent the SGS model. A more detailed and rigorous description can be found in [25, 30].

A severe limitation on the use of the SGS model is that the chosen closure relations and, in fact, the very concept of SGS turbulence energy only applies if the velocity fluctuations on subgrid scales are nearly isotropic. This limits the LES methodology to flows where all anisotropies stemming from large scale features, like boundary conditions or external forces, can be resolved. In the *FEARLESS* method, the grid resolution is locally adjusted by adaptive mesh refinement (AMR) in order to ensure that the anisotropic, energy-containing scales are resolved everywhere. In this way, it is assumed that turbulence is asymptotically isotropic on length scales comparable to or less than the grid resolution. It is very difficult to justify the latter assumption *a priori*, because there are no refinement criteria that would guarantee asymptotic isotropy on the smallest resolved length scales. By a case-by-case careful analysis of simulation results, however, one can gain confidence whether AMR resolves turbulent regions appropriately.

3 Resolving the Turbulent Flow with AMR

In a first group of works, only the novel AMR criteria described in Sect. 2 were tested and applied to hydrodynamical simulations relevant for the physics of galaxy cluster evolution.

Firstly, 3D hydrodynamical simulations were performed in an idealized setup, representing a moving subcluster during a merger event [23]. Whereas AMR simulations performed with the usual refinement criteria based on local gradients of temperature and density do not properly resolve the production of turbulence in the subcluster wake, the new criteria provide a better resolution of this flow, allowing to follow the onset of the shear instability, the evolution of the turbulent wake and the subsequent back-reaction on the subcluster core morphology.

The merging events, studied in the previous work in a simplified fashion, have been further investigated by means of full cosmological simulations, starting from realistic initial conditions [7]. In this case, the refinement criteria based on regional variability of control variables of the flow are used together with the customary overdensity criteria for baryons and dark matter. This approach is effective in resolving turbulent flows in the ICM, with a turbulent velocity in the cluster core larger than 200 km s^{-1} and a turbulent pressure contribution at the percent level. Further details, especially from the computational side, were already given in our project intermediate report [21].

The recent study of major merger events performed in the framework of this project [24] is somehow complementary to the minor merger scenario presented above. Although this problem has been already addressed several times in the last years [17, 31–37], the novel tools developed for the study of turbulent flows allowed to focus on the propagation of merger shocks and their role in injecting turbulence in the ICM, in particular in the post-shock region. Emphasis will be thus mainly put on quantitative and morphological features of merger shocks and the subsequently generated turbulence in ICM. Turbulence in the post-shock region is likely to be related with magnetic field amplification and CR acceleration, and consequently can be linked with cluster radio observations.

We performed a series of cosmological simulations of cluster mergers, based on a flat ΛCDM background cosmology with parameters $\Omega_\Lambda = 0.7$, $\Omega_\mathrm{m} = 0.3$, $\Omega_\mathrm{b} = 0.04$, $h = 0.7$, $\sigma_8 = 0.9$, and $n = 1$. The simulations have been initialized at redshift $z_\mathrm{in} = 60$ using the [38] transfer function, and evolved to $z = 0$. Cooling physics, feedback and transport processes are neglected. An ideal equation of state was used for the gas, with $\gamma = 5/3$.

The simulation box has a comoving size of 128 Mpc h^{-1}. It is resolved with a root grid (AMR level $l = 0$) of 64^3 cells and 64^3 N-body particles. The mass of each particle in this grid is $8.3 \times 10^{11}\ M_\odot$. A static grid ($l = 1$) was nested inside the root grid. It has a size of 64 Mpc h^{-1} and was resolved in 64^3 cells and 64^3 particles (particle mass $1.03 \times 10^{11}\ M_\odot$). Inside this grid, in a volume with side of 38.4 Mpc h^{-1}, a further static grid ($l = 2$) is added, and grid refinement from level $l = 3$ to $l = 6$ is enabled. The linear refinement factor N is set to 2, allowing an effective spatial resolution of 31.25 kpc h^{-1} at the maximum refinement level. The static grids and the region where AMR is allowed are nested on the location of a cluster merger, identified in a DM-only low-resolution run. Seven representative major mergers were chosen in our volume, focusing on events occurring at $0.25 < z < 0.7$ between halos with mass $M > 10^{13}\ M_\odot$, and with a mass ratio between the merging clumps larger than 0.5.

The morphological evolution of a representative merger is shown in Fig. 2 through the evolution of temperature. The two subclumps approach each other almost head-on, with a relative velocity of 980 km s^{-1}, and merge at $z \simeq 0.3$. A web of filaments is visible around the forming structure, as density contours. The gas in the ICM is severely attracted in the newly formed potential well, generating a shock wave which propagates through the cluster. Part of the kinetic and gravitational energy of the merger event is thus dissipated into the ICM. As the shock propagates

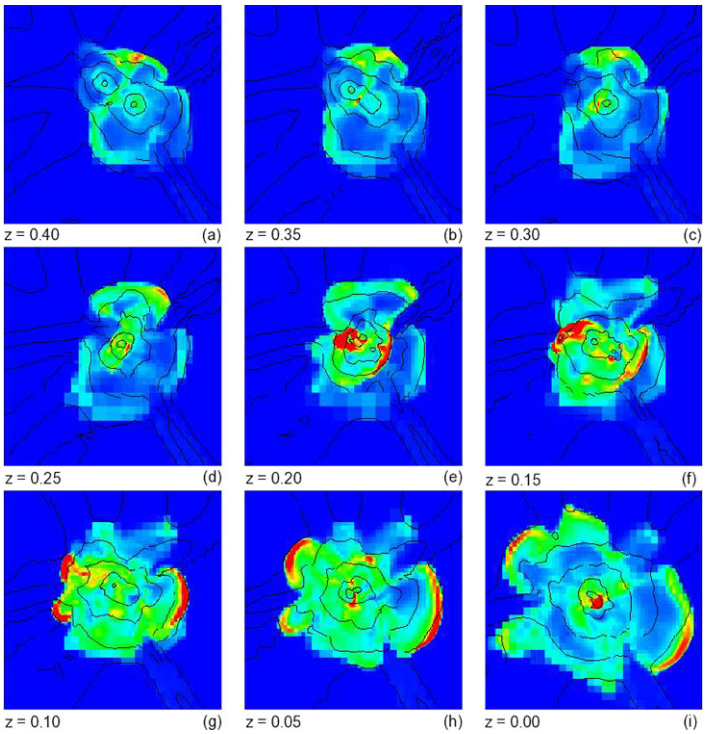

Fig. 2 The evolution of a merger event is shown in slices of temperature. The redshift is indicated at the lower left of each panel, and a identification letter is at the lower right. Each panel has a size of $7.7 \times 7.7\,\mathrm{Mpc}\ h^{-1}$ and is parallel to the yz plane. Temperature is color coded, with density contours overlayed. The highest temperature value of the scale (red) corresponds to $3.8 \times 10^7\,\mathrm{K}$

outwards, it interacts with the surrounding filaments and is broken in separate sections, as clearly visible in the bottom row of Fig. 2.

The propagation velocity of the shock is up to $1500\,\mathrm{km\ s^{-1}}$, corresponding to Mach numbers initially in the range from 2.5 to 7. The maximum temperature in the cluster region exceeds $10^8\,\mathrm{K}$ at $z = 0.2$, several times larger than the cluster virial temperature (about $3 \times 10^7\,\mathrm{K}$).

The estimated size of the post-shock region along the direction of shock propagation is of the order of $300\,\mathrm{kpc}\ h^{-1}$, with the velocity dispersion larger than $100\,\mathrm{km\ s^{-1}}$. The time scale for the shock propagation is about 2 Gyr. Within this time after the major merger, the ratio of turbulent to total pressure at the cluster center is larger than 10%, and still larger than that of a relaxed cluster simulated for comparison, until $z = 0$.

A very interesting similarity in morphology can be noticed between our simulations and some observed clusters with mergers ongoing, like for example the Mpc-scale giant arc seen in the radio observations of A3376 [39]. Besides the morphological similarities, the physical link between the radio emission and the turbulence injected in the post-shock region lies in the assumption of the coupling of

the compressional modes resolved in the hydrodynamic turbulence and the Alfvénic turbulence, needed for particle acceleration according to the Fermi mechanism. The radio morphology matches the morphology of the simulated structure in temperature and, more importantly, in vorticity, which traces turbulence. Of course, a more detailed comparison should make use of more sophisticated tools for converting the information from the hydrodynamical simulations in synthetic observations; this is left for future work.

From the computational point of view, the choice of a refinement criterion and of its relevant thresholds and parameters is a very delicate task in AMR simulations. Cosmological simulations of galaxy clusters are favored by the clumped behavior of these objects: criteria based on baryon or dark matter overdensity, when properly set, are able to catch the relevant structures with a good compromise between accuracy and saving of computational resources [40, 41]. Unfortunately the simulations presented in this work are extremely challenging from this point of view, because we are mainly interested in the evolution of a shocked region, whose size at late times is comparable with the cluster size, and that for our purpose should be carefully refined.

A typical run, with root resolution of 64^3 grid cells and N-body particles, two nested static grids and the AMR to $l = 6$, consumes from 1000 to 2000 CPU-h on 128 CPUs of the SGI Altix 4700 *HLRB II*, depending on the merger evolution. Doubling the root grid resolution was not computationally convenient (see also the comment on the code issues at the end of Sect. 4), whereas a simulation with the same setup and a root resolution of 96^3, used for a resolution study, runs in about 10000 CPU-h on 128 CPUs.

4 FEARLESS Simulation of a Galaxy Cluster

The full *FEARLESS* approach, briefly presented in Sect. 2, is applied in [30] to cosmological simulations of the formation and evolution of a galaxy cluster. This work has been performed jointly with the computational resources granted to this project and to *h0972*.

Two simulations with and without the subgrid scale model are compared in detail. The simulations were done using a flat ΛCDM background cosmology with a dark energy density $\Omega_\Lambda = 0.7$, a total (including baryonic and dark matter) matter density $\Omega_\mathrm{m} = 0.3$, a baryonic matter density $\Omega_\mathrm{b} = 0.04$, the Hubble parameter set to $\mathrm{h} = 0.7$, the mass fluctuation amplitude $\sigma_8 = 0.9$, and the scalar spectral index $n = 1$. Both simulations were started with the same initial conditions at redshift $z_\mathrm{in} = 60$, using the [38] transfer function, and evolved to $z = 0$. The simulations are adiabatic with a heat capacity ratio $\gamma = 5/3$ assuming a fully ionized gas with a mean molecular weight $m_\mu = 0.6\,u$. Cooling physics, magnetic fields, feedback, and transport processes are neglected.

The simulation box has a comoving size of $128\,\mathrm{Mpc}\,h^{-1}$. It is resolved with a root grid (level $l = 0$) of 128^3 cells and 128^3 N-body particles. A static child grid

($l = 1$) is nested inside the root grid with a size of 64 Mpc h^{-1}, 128^3 cells and 128^3 N-body particles. The mass of each particle in this grid is $9 \times 10^9 M_\odot\ h^{-1}$. Inside this grid, in a volume of 38.4 Mpc h^{-1}, adaptive grid refinement from level $l = 2$ to $l = 7$ is enabled using the overdensity refinement criterion as described in [7] with an overdensity factor $f = 4.0$. The refinement factor between two levels was set to 2, allowing for an effective resolution of 7.8 kpc h^{-1}.

The static and dynamically refined grids were nested around the place of formation of a galaxy cluster, identified using the HOP algorithm [42]. The cluster has a virial mass of $M_{\rm vir} = 5.95 \times 10^{14} M_\odot\ h^{-1}$ and a virial radius of $R_{\rm vir} = 1.37$ Mpc h^{-1}.

In Fig. 3 a short time series of density and turbulent velocity slices is presented, and several merger events in the cluster outskirts can be identified (for example, in the rectangle in panel 3*a*). A considerable amount of turbulent energy is localized in front and in the wake of the merging clumps (panels 3*b* and *d*). From this point of view, the distribution of turbulent energy traces the local merging history of a galaxy cluster, until it is dissipated into internal energy completely. The morphological evolution of the cluster gives a clear sense of the markedly local behavior of the production and dissipation of turbulence.

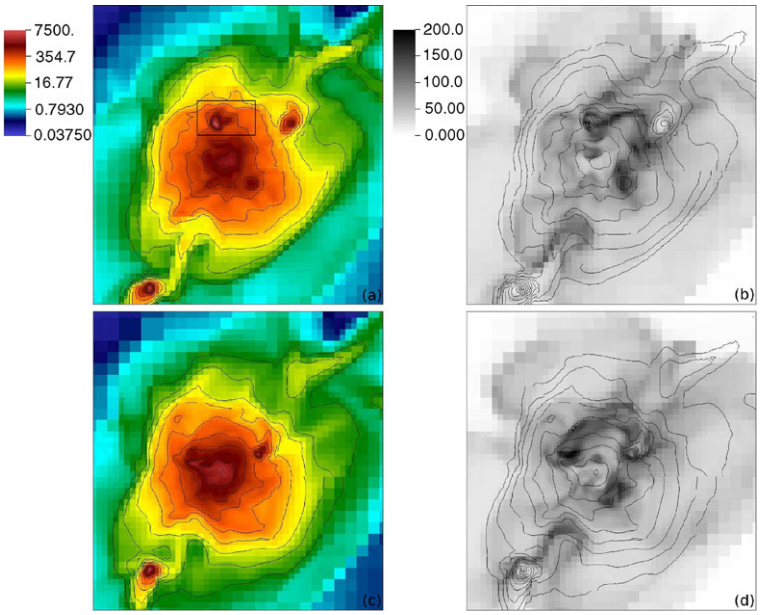

Fig. 3 Slices of baryon density (left-hand panels, *a* and *c*) and turbulent velocity $q = \sqrt{2e_{\rm t}}$ (right-hand panels, *b* and *d*) at different redshifts z, for the cosmological simulation run with *FEARLESS*. The density is logarithmically color coded as overdensity with respect to the average baryon density in the colorbar on the left of panel *a*, whereas q is linearly coded in km s^{-1}, according to the colorbar on the left of panel *b*. The overlayed contours show density. The slices show a region of 6.4×6.4 Mpc h^{-1} around the center of the main cluster followed in the simulation. Panels *a* and *b* refer to $z = 0.05$, panels *c* and *d* to $z = 0$

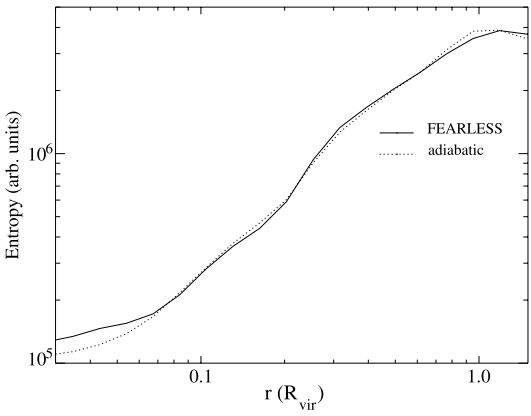

Fig. 4 Radial profiles of mass-weighted entropy (defined in the text) at $z = 0$. The dotted line refers to the simulation without SGS model, whereas the solid line is for the *FEARLESS* simulation

The merger events contribute therefore to the cluster energy budget, at the location where the turbulent dissipation modeled in *FEARLESS* is added to the numerical dissipation of the numerical scheme. Since the flow in the ICM is subsonic, the global turbulent energy contribution at the unresolved length scales is however smaller than 1% of the internal energy.

Another interesting result comes from the comparison between radial profiles in the *FEARLESS* simulation and in the standard adiabatic run, and is the change in the temperature and density profiles at the cluster center. In particular, in the *FEARLESS* run T is larger (3%) for central distances $r < 0.07\ R_{\rm vir}$, with respect to the standard run. Consequently the core in that run is less dense, so that the ICM remains in hydrostatic equilibrium. The local energy budget in the cluster core is therefore modified by the SGS model. This change is more clearly reflected on the entropy which is defined, as is customary in astrophysics, as

$$K = \frac{T}{\rho^{\gamma-1}} \tag{3}$$

with $\gamma = 5/3$ and ρ is the gas density. The entropy in the cluster core is higher in the *FEARLESS* run as compared to the standard run (Fig. 4). This result is consistent both with the locally increased dissipation of turbulent to internal energy provided by the SGS model and with the higher degree of mixing induced in the cluster core, as evaluated by the local velocity dispersion (cf. [30] for more details).

The level on entropy in cluster cores has been long debated, in particular for the discrepant results between SPH and grid codes [4, 43, 44]. Recently, [45] pointed out that the core temperature and entropy in grid-based codes are affected by a spurious increase, caused by the N-body noise in the gravitational force field. In our opinion, the higher entropy core value in the FEARLESS run suggests that the typical flat entropy core is a hydrodynamical feature which requires a better understanding of the numerics in mesh codes, and is at least not primarily caused by N-body noise. Further investigations are certainly needed on this issue.

From the computational viewpoint, the SGS model in *FEARLESS* does not increase significantly the use of CPU time ($\sim +20\%$). These simulations were run on the SGI Altix 4700 *HLRB II* on 128 CPUs, with a typical consumption time of 1100 and 1350 CPU-h for the adiabatic and *FEARLESS* simulations, respectively. A large part of the development and testing work was done with this resolution, although one could argue, from the rather small consumption of resources, that a higher root grid resolution could have been used for the production runs. Unfortunately, this is not the case, basically for known inefficiencies of the code ENZO, v.1.0, in managing the output and the memory. The implementation of structured AMR in the code [46] produces, at every data dump, one file for each grid patch produced, and the run performance decreases dramatically for more than about 10000 grids (about 2600 are produced in our runs). The new release (v.1.5) of the ENZO code overcomes this inefficiency by producing one output file for each CPU, so we expect to make a more efficient use of the available computational resources in our future work.

5 Conclusions and Outlook

Large Eddy Simulations (LES) are based on the notion of filtering the fluid dynamic equations at a specific length scale, thus performing a scale separation between the resolved and the unresolved flow. The latter is treated by means of a subgrid scale model, which in turn is coupled to the hydrodynamical equations governing the former. In principle, a single scale separation is not practical in simulations of clumped media, and furthermore it is not compatible with the concept of adaptive mesh refinement (AMR), often used to study astrophysical phenomena. The solution proposed to this problem is the development of a new numerical scheme that uses AMR and LES in combination, which was called *FEARLESS*.

The initial aim of the present project was to address the numerical problem of turbulence modeling in galaxy clusters, by focusing in particular on the AMR methods (Sect. 3). With the extension of our project, the work made a further step, applying the full *FEARLESS* scheme to simulations of galaxy clusters (Sect. 4). The novel tool appears suitable for modeling turbulent flows over a wide range of length scales, a key feature in the treatment of many astrophysical flows including the intracluster medium. The results give rise to several interesting implications with regard to the physics of galaxy clusters and to the numerical methods employed for their exploration in computational cosmology.

Future research with *FEARLESS* in the cluster physics will include a follow-up of [24] with the full numerical scheme; this study is particularly interesting because the turbulent energy injected by mayor mergers has a significant role in the energy budget, with respect to minor mergers. It will be also important to explore the turbulent flows not only in the ICM, but also in colder baryon phases like the Warm-Hot Intergalactic Medium ($10^5\,\mathrm{K} < T < 10^7\,\mathrm{K}$). The cosmic filaments and the cluster outer regions consist of baryons in this temperature range, and knowledge of the

turbulent state of this gas is potentially important for shaping the emission and absorption lines associated with it (see [47] for a review).

Also the development work associated with *FEARLESS* is still in progress. The current version of the SGS model has to be considered as an intermediate solution to address some basic questions related to dynamics of the turbulent intra-cluster medium. A more elaborate model that is able to handle the complexity of the flow (wide range of Mach numbers and large density gradients as well as pronounced inhomogeneities) in simulations of large scale structure evolution is under development (also see the contribution on *Numerical Models of Turbulence in Isothermal and Thermally Bistable Interstellar Gas* [48] in this volume). The infrastructure for the further development is the new release 1.5 of the ENZO code, which fixes many of the numerical inefficiencies we described. The first application reviewed here shows the promising perspectives for the use of an SGS model in combination with AMR, and its potential impact on many branches of numerical astrophysics.

Acknowledgements Thanks to the whole support team of the Leibniz Rechenzentrum for their invaluable help during our work.

References

1. J.P. Ostriker, ARA&A **31**, 689 (1993)
2. M.L. Norman, G.L. Bryan, LNP Vol. 530: The Radio Galaxy Messier 87 **530**, 106 (1999)
3. R.A. Sunyaev, M.L. Norman, G.L. Bryan, Astronomy Letters **29**, 783 (2003)
4. K. Dolag, F. Vazza, G. Brunetti, G. Tormen, *Mon. Not. Roy. Soc.* **364**, 753 (2005)
5. M. Brüggen, M. Hoeft, M. Ruszkowski, *Astrophys. J.* **628**, 153 (2005)
6. P. Rebusco, E. Churazov, R. Sunyaev, H. Böhringer, W. Forman, MNRAS **384**, 1511 (2008)
7. L. Iapichino, J.C. Niemeyer, *Mon. Not. Roy. Soc.* **388**, 1089 (2008)
8. K. Dolag, M. Bartelmann, H. Lesch, *Astron. Astrophys.* **387**, 383 (2002)
9. M. Brüggen, M. Ruszkowski, A. Simionescu, M. Hoeft, C. Dalla Vecchia, ApJ **631**, L21 (2005)
10. K. Subramanian, A. Shukurov, N.E.L. Haugen, *Mon. Not. Roy. Soc.* **366**, 1437 (2006)
11. A.R. Bell, *Mon. Not. Roy. Soc.* **353**, 550 (2004)
12. F. Miniati, T.W. Jones, H. Kang, D. Ryu, ApJ **562**, 233 (2001)
13. F. Miniati, D. Ryu, H. Kang, T.W. Jones, ApJ **559**, 59 (2001)
14. G. Brunetti, A. Lazarian, *Mon. Not. Roy. Soc.* **378**, 245 (2007)
15. M.L. Norman, ArXiv Astrophysics e-prints, astro-ph/0402230 (2004)
16. O. Agertz, B. Moore, J. Stadel, D. Potter, F. Miniati, J. Read, L. Mayer, A. Gawryszczak, A. Kravtsov, A. Nordlund, F. Pearce, V. Quilis, D. Rudd, V. Springel, J. Stone, E. Tasker, R. Teyssier, J. Wadsley, R. Walder, MNRAS **380**, 963 (2007)
17. N.L. Mitchell, I.G. McCarthy, R.G. Bower, T. Theuns, R.A. Crain, *Mon. Not. Roy. Soc.* **395**, 180 (2009)
18. B.W. O'Shea, G. Bryan, J. Bordner, M.L. Norman, T. Abel, R. Harkness, A. Kritsuk, in *Adaptive Mesh Refinement – Theory and Applications, ed. T. Plewa, T. Linde, V.G. Weirs (Berlin; New York: Springer)*, *Lecture Notes in Computational Science and Engineering*, vol. 41 (2005), p. 341
19. P. Woodward, P. Colella, Journal of Computational Physics **54**, 115 (1984)
20. G.L. Bryan, M.L. Norman, J.M. Stone, R. Cen, J.P. Ostriker, Computer Physics Communications **89**, 149 (1995)

21. L. Iapichino, J.C. Niemeyer, J. Adamek, S. Paul, M. Scuderi, in *High Performance Computing in Science and Engineering, Garching/Munich 2007*, ed. by S. Wagner, M. Steinmetz, A. Bode, M. Brehm (2009), pp. 45–56
22. W. Schmidt, C. Federrath, M. Hupp, S. Kern, J.C. Niemeyer, *Astron. Astrophys.* **494**, 127 (2009)
23. L. Iapichino, J. Adamek, W. Schmidt, J.C. Niemeyer, *Mon. Not. Roy. Soc.* **388**, 1079 (2008)
24. S. Paul, L. Iapichino, F. Miniati, J. Bagchi, K. Mannheim, ArXiv e-prints (2010), 1001.1170, submitted to ApJ
25. W. Schmidt, J.C. Niemeyer, W. Hillebrandt, *Astron. Astrophys.* **450**, 265 (2006)
26. T.W. Jones, in *Extragalactic Jets: Theory and Observation from Radio to Gamma Ray*, *ASP Conference Series*, vol. 386, ed. by T. Rector, D. De Young (2007), p. 398, arXiv e-prints: 0708.2284
27. M. Lesieur, O. Metais, Annual Review of Fluid Mechanics **28**, 45 (1996)
28. M. Germano, Journal of Fluid Mechanics **238**, 325 (1992)
29. A. Favre, SIAM: Problems of hydrodynamics and continuum mechanics pp. 231–266 (1969)
30. A. Maier, L. Iapichino, W. Schmidt, J.C. Niemeyer, *Astrophys. J.* **707**, 40 (2009)
31. K. Roettiger, J. Burns, C. Loken, ApJ **407**, L53 (1993)
32. K. Roettiger, J.O. Burns, C. Loken, *Astrophys. J.* **473**, 651 (1996)
33. K. Roettiger, C. Loken, J.O. Burns, *Astrophys. J. Suppl.* **109**, 307 (1997)
34. P.M. Ricker, C.L. Sarazin, *Astrophys. J.* **561**, 621 (2001)
35. H. Mathis, G. Lavaux, J.M. Diego, J. Silk, *Mon. Not. Roy. Soc.* **357**, 801 (2005)
36. G.B. Poole, M.A. Fardal, A. Babul, I.G. McCarthy, T. Quinn, J. Wadsley, *Mon. Not. Roy. Soc.* **373**, 881 (2006)
37. G.B. Poole, A. Babul, I.G. McCarthy, M.A. Fardal, C.J. Bildfell, T. Quinn, A. Mahdavi, *Mon. Not. Roy. Soc.* **380**, 437 (2007)
38. D.J. Eisenstein, W. Hu, ApJ **511**, 5 (1999)
39. J. Bagchi, F. Durret, G.B.L. Neto, S. Paul, Science **314**(5800), 791 (2006)
40. B.W. O'Shea, K. Nagamine, V. Springel, L. Hernquist, M.L. Norman, *Astrophys. J. Suppl.* **160**, 1 (2005)
41. K. Heitmann, Z. Lukić, P. Fasel, S. Habib, M.S. Warren, M. White, J. Ahrens, L. Ankeny, R. Armstrong, B. O'Shea, P.M. Ricker, V. Springel, J. Stadel, H. Trac, Computational Science and Discovery **1**(1), 015003 (2008)
42. D.J. Eisenstein, P. Hut, *Astrophys. J.* **498**, 137 (1998)
43. J.W. Wadsley, G. Veeravalli, H.M.P. Couchman, *Mon. Not. Roy. Soc.* **387**, 427 (2008)
44. D. Kawata, T. Okamoto, R. Cen, B.K. Gibson, ArXiv e-prints (2009), 0902.4002
45. V. Springel, *Mon. Not. Roy. Soc.* **401**, 791 (2010)
46. M.J. Berger, P. Colella, Journal of Computational Physics **82**, 64 (1989)
47. S. Bertone, J. Schaye, K. Dolag, Space Science Reviews p. 28 (2008)
48. W. Schmidt, D. Seifried, M. Niklaus, J. Niemeyer, (2010). (in this volume)